Light transmission along dispersive plasmonic gap and its subwavelength guidance characteristics

Ki Young Kim, Young Ki Cho, and Heung-Sik Tae

School of Electrical Engineering and Computer Science, Kyungpook National University, Daegu 702-701, Korea

doors@ee.knu.ac.kr

http://palgong.knu.ac.kr/~doors

Jeong-Hae Lee

Department of Radio Science and Communication Engineering, Hongik University, Seoul 121-791, Korea

Abstract: Light transmission along dispersive plasmonic gap with varied gap widths and its subwavelength guidance characteristics are numerically investigated over a wide frequency range. Mode numbers for each guided modes of the dispersive plasmonic gaps are properly assigned in order to be in consistency with the parallel plate waveguide composed of the perfect electric conductor. Overall and salient features of the role of the gap widths on the guided propagation characteristics are clearly understood by investigating several dispersion curves of varied gap widths. Cutoff frequency downshifts of the dispersive plasmonic gap compared with the perfect electric conductor based parallel plate waveguides are also observed. Finally, surface plasmon polariton modes having subwavelength guidance capability are described in more detail, which are directly governed by the plasmonic property of the metals. The results are expected to be utilized in designing various potential subwavelength nanophotonic devices.

OCIS codes: (130.2790) Guided waves; (240.5420) Polaritons; (240.6680) Surface plasmons; (260.2030) Dispersion; (350.5500) Propagation.

References and links

1. Focus Issue: Extraordinary Light Transmission Through Sub-Wavelength Structured Surfaces, Opt. Express **12**, 3618-3706 (2004).
2. T. W. Ebbesen, H. J. Lezec, H. F. Ghaemi, T. Thio, and P. A. Wolff, "Extraordinary optical transmission through sub-wavelength hole arrays," Nature **391**, 667-669 (1998).
3. H. A. Bethe, "Theory of diffraction by small holes," Phys. Rev. **66**, 163-182 (1944).
4. C. J. Bouwkamp, "On Bethe's theory of diffraction by small holes," Philips Res. Rep. **5**, 321-332 (1950)
5. C. J. Bouwkamp, "Diffraction theory," Rep. Prog. Phys. **17**, 35-100 (1954).
6. W. L. Barnes, A. Dereux, and T. W. Ebbesen, "Surface plasmon subwavelength optics," Nature **424**, 824-830 (2003).
7. J. A. Porto, F. J. García-Vidal, and J. B. Pendry, "Transmission resonances on metallic gratings with very narrow slits," Phys. Rev. Lett. **83**, 2845-2848 (1999).
8. F. J. García-Vidal, E. Moreno, J. A. Porto, and L. Martín-Moreno, "Transmission of light through a single rectangular hole," Phys. Rev. Lett. **95**, 103901 (2005).
9. S. A. Maier, "Gain-assisted propagation of electromagnetic energy in subwavelength surface plasmon polariton gap waveguides," Opt. Comm. (to be published).
10. G. Veronis and S. Fan, "Bends and splitters in metal-dielectric-metal subwavelength plasmonic waveguides," Appl. Phys. Lett. **87**, 131102 (2005).
11. H. Shin, P. B. Catrysse, and S. Fan, "Effect of the plasmonic dispersion relation on the transmission properties of subwavelength cylindrical holes," Phys. Rev. B **72**, 085436 (2005).
12. R. Gordon and A. G. Brolo, "Increased cut-off wavelength for a subwavelength hole in a real metal," Opt. Express **13**, 1933-1938 (2005).

#9300 - $15.00 USD Received 28 October 2005; revised 30 November 2005; accepted 21 December 2005

13. D. –K. Qing and G. Chen, "Nanoscale optical waveguides with negative dielectric cladding," Phys. Rev. B **71**, 153107 (2005).
14. R. Zia, M. D. Selker, P. B. Catrysse, and M. Brongersma, "Geometries and materials for subwavelength surface plasmon modes," J. Opt. Soc. Am. A **21**, 2442-2446 (2004).
15. A. J. Lichtenberg and J. R. Woodyard, "Plasma waveguides as low loss structures," J. Appl. Phys. **33**, 1976-1979 (1962).
16. C. Davis and T. Tamir, "Surface and interface waves in plasma gaps," J. Appl. Phys. **37**, 461-462 (1966).
17. A. A. Oliner and T. Tamir, "Backward waves on isotropic plasma slabs," J. Appl. Phys. **33**, 231-233 (1962).
18. E. N. Economou, "Surface plasmons in thin films," Phys. Rev. **182**, 539-554 (1969).
19. T. Takano and J. Hamasaki, "Propagating modes of a metal-clad-dielectric slab waveguide for integrated optics," IEEE J. Quantum Elec. **8**, 206-212 (1972).
20. K. Nosu and J. Hamasaki, "The influence of the longitudinal plasma wave on the propagation characteristics of a metal-clad-dielectric-slab waveguide," IEEE J. Quantum. Electron. **12**, 745-748 (1976).
21. B. Prade, J. Y. Vinet, and A. Mysyrowicz, "Guided optical waves in planar heterostructures with negative dielectric constant," Phys. Rev. B **44**, 13556-13572 (1991).
22. K. Tanaka and M. Tanaka, "Simulations of nanometric optical circuits based on surface plasmon polariton gap waveguide," Appl. Phys. Lett. **82**, 1158-1160 (2003).
23. B. Wang and G. P. Wang, "Metal heterowaveguides for nanometric focusing of light," Appl. Phys. Lett. **85**, 3599-3601 (2004).
24. G. D'Aguanno, N. Mattiucci, M. Scalora, and M. J. Bloemer, "TE and TM guided modes in an air waveguide with negative-index-material cladding," Phys. Rev. E **71**, 046603 (2005).
25. M. M. Sigalas, C. T. Chan, K. M. Ho, and C. M. Soukoulis, "Metallic photonic band-gap materials," Phys. Rev. B **52**, 11744-11751 (1995).
26. L. –M. Li, Z. –Q. Zhang, and X. Zhang, "Transmission and absorption properties of two-dimensional metallic photonic-band-gap materials," Phys. Rev. B **58**, 15589-15594 (1998).
27. X. Zhang, "Image resolution depending on slab thickness and object distance in a two-dimensional photonic-crystal-based superlens," Phys. Rev. B **70**, 195110 (2004).
28. X. Zhang, "Absolute negative refraction and imaging of unpolarized electromagnetic waves by two-dimensional photonic crystals," Phys. Rev. B **70**, 205102 (2004).
29. X. Zhang and L. –M. Li, "Creating all-angle-negative refraction by using insertion," Appl. Phys. Lett. **86**, 121103 (2005).
30. X. Zhang, "Effect of interface and disorder on the far-field image in a two-dimensional photonic-crystal-based flat lens," Phys. Rev. B **71**, 165116 (2005).
31. X. Zhang, "Subwavelength far-field resolution in a square two-dimensional photonic crystal," Phys. Rev. E **71**, 037601 (2005).
32. X. Zhang, "Tunable non-near-field focus and imaging of an unpolarized electromagnetic wave," Phys. Rev. B **71**, 235103 (2005).
33. Yu. M. Aliev, H. Schlüter, and A. Shivarova, *Guided-Wave-Produced Plasmas* (Springer-Verlag, Heidelberg, 2000), Chap. 3.
34. D. H. Staelin, A. W. Morgenthaler, and J. A. Kong, *Electromagnetic Waves* (Prentice-Hall Inc., New York, 1994), Chap. 7.
35. W. P. Allis, S. J. Buchsbaum, and A. Bers, *Waves in Anisotropic Plasmas* (The MIT Press, Cambridge, 1963), Chap. 10.
36. L. Novotny and C. Hafner, "Light propagation in a cylindrical waveguide with a complex, metallic, dielectric function," Phys. Rev. E **50**, 4094-4106 (1994).
37. A. D. Rakić, A. B. Djurišić, J. M. Elazar, and M. L. Majewski, "Optical properties of metallic films for vertical-cavity optielectronic devices," Appl. Opt. **37**, 5271-5283 (1998).
38. T. Tamir and A. A. Oliner, "The spectrum of electromagnetic waves guided by a plasma layer," Proc. IEEE **51**, 317-332 (1963).
39. V. L. Granatstein, S. P. Schlesinger, A. Vigants, "The open plasmaguide in extremes of magnetic field," IEEE Trans. Antennas Propag. **11**, 489-496 (1963).
40. T. Tamir and S. Palócz, "Surface waves on plasma-clad metal rods," IEEE Trans. Microwave Theory Tech. **12**, 189-196 (1964).
41. P. Tournois and V. Laude, "Negative group velocities in metal-film optical waveguides," Opt. Commun. **137**, 41-45 (1997).
42. K. Y. Kim, J. –H. Lee, Y. K. Cho, and H. –S. Tae, "Electromagnetic wave propagation through doubly dispersive subwavelength metamaterial hole," Opt. Express, **13**, 3653-3665 (2005),
43. I. V. Shadrivov, A. A. Sukhorukov, and Y. S. Kivshar, "Guided modes in negative-refractive-index waveguides," Phys. Rev. E **67**, 057602 (2003).
44. I. V. Shadrivov, A. A. Sukhorukov, Y. S. Kivshar, A. A. Zharov, A. D. Boardman, and P. Egan, "Nonlinear surface waves in left-handed materials," Phys. Rev. E **69**, 016617 (2004).
45. J. Schelleng, C. Monzon, P. F. Loschialpo, D. W. Forester, and L. N. Medgyesi-Mitschang, "Characteristics of waves guided by a grounded "left-handed" material slab of finite extent," Phys. Rev. E **70**, 066606 (2004).
46. H. –G. Unger, *Planar Optical Waveguides and Fibers* (Clarendon Press, Oxford, 1977).
47. D. Marcuse, *Theory of Dielectric Optical Waveguides*, 2nd ed. (Academic Press, San Diego, 1991).

#9300 - $15.00 USD Received 28 October 2005; revised 30 November 2005; accepted 21 December 2005

1. Introduction

Enhanced light transmissions through subwavelength single/periodic slits or apertures on metallic surfaces have become the focus of extensive study (for instance, see ref. [1] and references therein), since Ebbesen's pioneering work on bidimensional periodic aperture arrays was first reported [2]. Such attention is not merely interest in challenging traditional tenets [3-5], but also related to the numerous potential nanophotonic applications, *e.g.*, optical data storage, near-field optical microscopy, and bio-photonics [6]. Conceptual qualitative explanations of the light transmission process through holes are identical for both single and arrayed apertures, where the illumination of aperture entrances by incident plane waves is coupled with the guided modes (eigenmode solutions) along the guided structures, then the guided modes decouple the electromagnetic energy into free space modes through the exit apertures. As such, these enhanced transmissions are strongly dependent on the guided modes along the guiding structure with a finite length between both ends [7, 8], making precise inspection of the subwavelength guided modes important and indispensable in analyzing these extraordinary physical phenomena.

In addition, the subwavelength guidance of light is also becoming more and more significant in its own right as regards potential applications in the building blocks of compact photonic devices [9-14]. The subwavelength guidance of light is known to be associated with the surface plasmon polariton (SPP), *i.e.*, the electromagnetic wave confined to the interface between materials with positive and negative permittivities. The negative permittivity of the guiding medium is due to the frequency dependent response of the medium to incident electromagnetic radiations. Plus, it is well known that the permittivities of metals at high frequencies (optical frequency regime) are usually negative below the plasma frequency, ω_p, as they are generally fitted to $\varepsilon(\omega) = 1 - \omega_p^2 / \omega^2$, which is the famous Drude model.

Accordingly, this paper investigates the guided electromagnetic waves along dispersive plasmonic gaps (DPGs) as one of the simplest candidates for the subwavelength guidance of light. A DPG is an air channel sandwiched by metals with infinite transverse extensions, *i.e.*, a parallel plate waveguide (PPW) using real metals with a plasmonic response. Analyses and applications of this type of electromagnetic or light wave guiding structure have already been reported by several other research teams. For example, Lichtenberg *et al*. focused on fast wave solutions for plasma waveguides with an infinite magnetic field along the structure and high-field linear accelerator applications [15]. In addition, the fast/slow, forward/backward, and TM/TE mode characteristics of a plasma gap have been briefly reported [16] in contrast to a plasma slab counterpart [17], where "real" plasmas were assumed. The dispersion relations of surface plasmons were investigated for single- and multiple-layered metal films, which included a metal-insulator-metal structure [18]. The guided modes and associated attenuation characteristics of metal-clad-dielectric-slab waveguides have also been reported [19, 20]. A more detailed study on the dispersion characteristics of metal-dielectric-metal heterostructures according to the frequency independent/dependent permittivity of the metal clad was presented by Prade *et al*.[21], and more recently, the SPP mode characteristics along negative dielectric cladding were reported with an emphasis on the development of a nanometric gap or subwavelength gap waveguide [9, 13, 14, 22, 23]. As a simple example of a waveguide with a negative refractive index (NRI) metamaterial, a PPW with NRI cladding has even been considered [24]. Nonetheless, when considering the definitive demands on photonic devices in the realm of nanophotonics or plasmonics, the subwavelength guidance of light by DPGs, as one of the simplest guiding structures, needs to be thoroughly investigated. However, previous work on the fundamental guided dispersion characteristics is still incomplete. In particular, discussions related to the gap width dependence on the dispersion characteristics are insufficient, which can be one of the most significant design guidelines for subwavelength guidance along DPGs.

Consequently, we concentrate on the dispersion characteristics of DPGs as variations of the gap width and obtain overall and salient pictures of the guided modes. Thus, the guided modes along DPGs, including the SPP modes as well as the PPW modes over a wide frequency range below and above the plasma frequency, are discussed with an emphasis on the dependence of

#9300 - $15.00 USD Received 28 October 2005; revised 30 November 2005; accepted 21 December 2005

the mode dispersion on the gap width variation. Brief comparisons with a PPW composed of a perfect electric conductor (PEC) are also made. Finally, the SPP modes with the gap dependences are contrasted. Even though we have chosen titanium-like plasmonic media as the cladding for the DPGs, this result can also be expected to be applied to other plasmonic media based DPGs and utilized to supply the guidelines for designing various compact photonic devices, as in ref. [10]. It should be noted that the Drude model used here is lossless, which can give physical insights into the behavior of real metals at optical frequencies.

2. Dispersive plasmonic gap waveguide and its characteristic equation

2.1 Dispersive plasmonic gap (DPG) waveguide

Figure 1 shows a schematic cutaway view of the DPG geometry and dielectric constant for the cladding employed in this work. In Fig. 1(a), the light guidance is performed in a $+z$ direction and the gap width is $2h$. The core region (region 1, $|x| < h$) is assumed to be air, and the dielectric constant of the cladding region (region 2, $|x| > h$) obeys the plasmonic response, such that $\varepsilon_{r2}(\omega) = 1 - \omega_p^2 / \omega^2$, where $\omega_p / 2\pi = 3600$ THz. This value is quite similar to that for titanium (Ti), and has been extensively utilized in other calculations [25-32]. (Practically, the collision frequency of Ti in ref. [25-32] is generally accepted as $\omega_c / 2\pi = 340$ THz. However, ω_c is relatively small compared with ω_p. Thus, it has a minimal affect on the dispersion characteristics and is disregarded here.) The dielectric constant for the air core region and magnetic constants for both regions are all assumed to be unity, *i.e.*, $\varepsilon_{r1} = \mu_{r1} = \mu_{r2} = 1.0$. As shown in Fig. 1(b), below the plasma frequency of $f_p = \omega_p / 2\pi = 3600$ THz, the dielectric constant is negative, whereas above the plasma frequency, the refractive index of the cladding, *i.e.*, $n_2 = (\mu_{r2}\varepsilon_{r2})^{1/2}$ becomes a positive real value and is plotted as a dashed line. The frequency at which $\varepsilon_{r2} = -1.0$ is referred to as the critical frequency and given by $f_c = f_p / \sqrt{2} = 2545.58$ THz, which plays a critical role in the dispersion characteristics, as discussed in the next section.

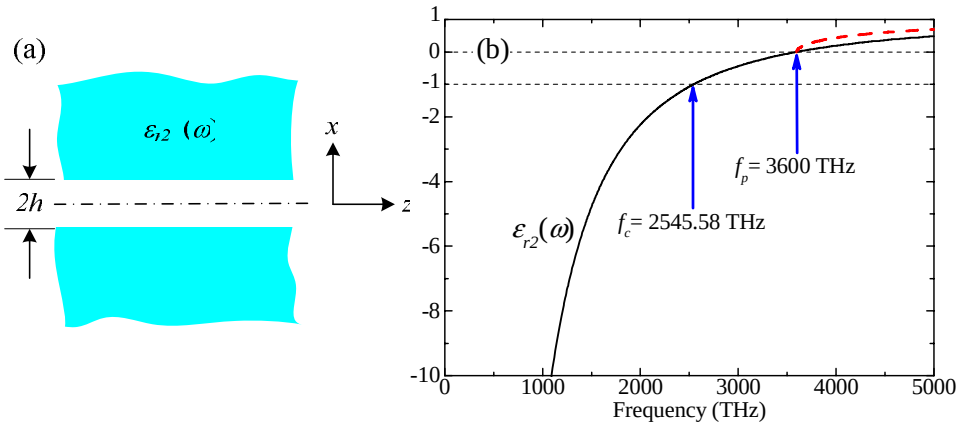

Fig. 1. (a) Schematic illustration of dispersive plasmonic gap (DPG) geometry and (b) dielectric constant of cladding.

2.2 Characteristic equations

The characteristic equations for DPG waveguiding systems can be easily derived in similar ways to the characteristic equations for metal-dielectric-metal waveguides [19], plasma slab waveguides [17, 33], and dielectric slab waveguides [34]. Yet, due to the negative dielectric cladding, mode numbers are assigned to each guided mode, which is different from the case of well known waveguides such as plasma and dielectric slabs, in order to be in consistent with the modes of a PPW with a PEC, which is theoretically the ideal version of DPGs. The tabulated characteristic equations for DPGs and their belongings are summarized in Table 1. Each equation can be easily obtained from the standard steps of boundary-value problems,

#9300 - $15.00 USD Received 28 October 2005; revised 30 November 2005; accepted 21 December 2005

where $k_i (i = 1, 2)$ is the transverse propagation constant for each region, k_0 is the free space wave number, and $\bar{\beta} (= \beta / k_0)$ is the normalized propagation constant in the propagation direction. Slow ($\beta > k_0$) and fast ($\beta < k_0$) wave modes, *i.e.*, SPP and PPW modes, respectively, both exist, however, the SPP modes only have a TM mode, as in the case of a plasma slab [17, 33], while the PPW modes include both TM and TE modes, as in the ideal case of a PPW with a PEC [34]. The characteristic equations for the SPP modes and PPW TE_m modes are identical to those for plasma slabs [17, 33] and dielectric slabs [34], respectively. In contrast, the mode numbers assigned to the PPW TM_m mode are the reverse of the case for dielectric slabs, due to the negative dielectric cladding.

Table 1. Characteristic equations for DPGs.

SPP mode $\left(\bar{\beta} > \mu_{r1}\varepsilon_{r1} (= 1.0)\right)$	PPW mode $\left(\bar{\beta} < \mu_{r1}\varepsilon_{r1} (= 1.0)\right)$	
TM_m	TM_m	TE_m
$m = 0$: $\frac{\varepsilon_{r2}}{\varepsilon_{r1}} \frac{k_1 h}{k_2 h} \tanh(k_1 h) + 1 = 0$	$m = 2, 4, 6, \cdots$: $\frac{\varepsilon_{r2}}{\varepsilon_{r1}} \frac{k_1 h}{k_2 h} \tan(k_1 h) - 1 = 0$	$m = 1, 3, 5, \cdots$: $\frac{\mu_{r2}}{\mu_{r1}} \frac{k_1 h}{k_2 h} \tan(k_1 h) - 1 = 0$
$m = 1$: $\frac{\varepsilon_{r2}}{\varepsilon_{r1}} \frac{k_1 h}{k_2 h} \coth(k_1 h) + 1 = 0$	$m = 1, 3, 5, \cdots$: $\frac{\varepsilon_{r2}}{\varepsilon_{r1}} \frac{k_1 h}{k_2 h} \cot(k_1 h) + 1 = 0$	$m = 2, 4, 6, \cdots$: $\frac{\mu_{r2}}{\mu_{r1}} \frac{k_1 h}{k_2 h} \cot(k_1 h) + 1 = 0$
$\begin{cases} k_1 = k_0 \left(\bar{\beta}^2 - \mu_{r1}\varepsilon_{r1}\right)^{1/2} \\ k_2 = k_0 \left(\bar{\beta}^2 - \mu_{r2}\varepsilon_{r2}\right)^{1/2} \end{cases}$	$\begin{cases} k_1 = k_0 \left(\mu_{r1}\varepsilon_{r1} - \bar{\beta}^2\right)^{1/2} \\ k_2 = k_0 \left(\bar{\beta}^2 - \mu_{r2}\varepsilon_{r2}\right)^{1/2} \end{cases}$	

3. Numerical results and discussion

3.1 Dispersion characteristics relative to variation of gap width

Figure 2 shows the dispersion characteristics of the DPG waveguides with six variations of the gap width, *i.e.*, $h = 50$, 25, 15, 10, 5, and 1nm, which were arbitrarily chosen for obvious contrast and to observe the evolution in relation to the gap width dependence. The shaded sections indicate the areas where no guided modes propagated. More detailed discussion on this will be available later. The TM_0 modes in the slow wave regions had no low-frequency cutoff and a high-frequency cutoff at the critical frequency of 2545.58 THz. In other words, the TM_0 mode only existed in the frequency region where the dielectric constant was smaller than the negative unity, which is interestingly identical to the case of a plasma slab [17] or plasma column [35]. From the fact that the TM_0 mode could exist even when the frequency was very low, this mode corresponded to the TEM mode of a PPW (composed of a PEC). Furthermore, in a lower frequency regime far away from the plasma frequency, the normalized propagation constants tended to be constant at slightly greater than unity, which means that a slow wave is supportable in this case. These deviations are due to the penetration of the fields into the cladding region. It is noted that such low frequency behaviors have been obviously resulted based on the lossless plasmonic response of the cladding. The modes using the lossless Drude model at lower frequencies are inconsistent to the real situation. Since an additional Lorentzian resonance effect was not added at the lower frequencies [36, 37], the use of the simpler plasmonic form of $\varepsilon(\omega) = 1 - \omega_p^2 / \omega^2$ allowed us to acquire valid physical insights in higher optical frequencies, *e.g.*, roughly above 600 THz.

The TM_0 mode also exhibited monotonically increasing dispersions with the frequency, representing its forward wave characteristics. Yet, as the frequency approached the critical frequency, the normalized propagation constant increased very rapidly.

#9300 - $15.00 USD Received 28 October 2005; revised 30 November 2005; accepted 21 December 2005

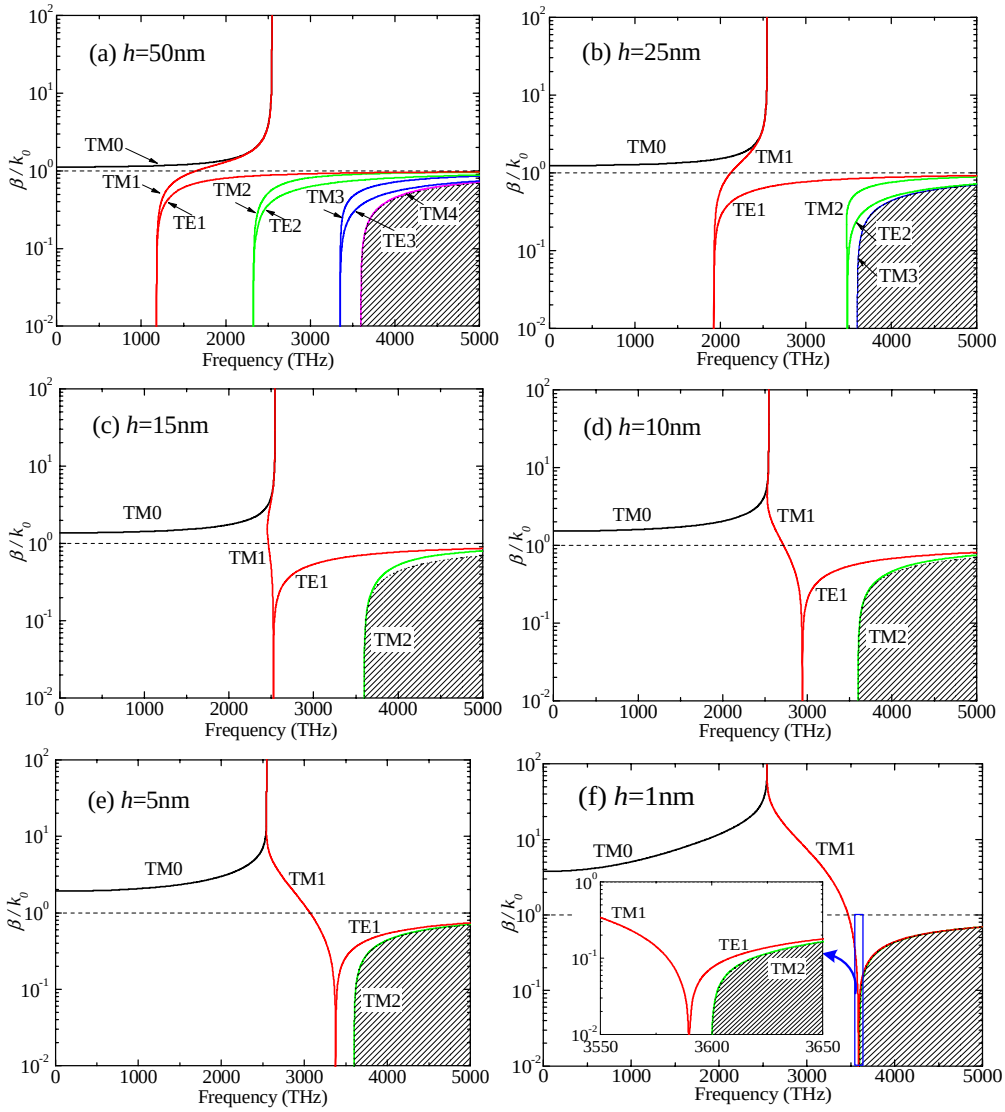

Fig. 2. Dispersion characteristics of DPG waveguides. (a) $h = 50$nm, (b) $h = 25$nm, (c) $h = 15$nm, (d) $h = 10$nm, (e) $h = 5$nm, and (f) $h = 1$nm.

In the case of a PPW with a PEC, the normalized propagation constant, $\bar{\beta}$, is equal to unity for the TM_0 (or, more generally, TEM) mode, where the phase velocity is the same as that for the light. The $\bar{\beta} = 1.0$ lines in Fig. 2 are shown as horizontal dashed lines, and also used for the border between the SPP and PPW modes (or between the slow and fast waves).

Another mode with a rapidly increased normalized propagation constant near the critical frequency was the TM_1 mode. Near the critical frequency, the normalized propagation constants for the TM_0 and TM_1 modes were nearly the same, at which point the phase velocity of the modes was extremely slow. In spite of the different characteristic equations for the SPP and PPW modes, as shown in Table 1, the curves for the TM_1 mode were observed to continue smoothly from the slow wave (SPP mode) region to the fast wave (PPW mode) region and finally cutoff, *i.e.*, $\bar{\beta} = 0$. As shown in Table 1, only the TM_1 mode had both SPP and PPW modes. The characteristic equation for the SPP TM_1 mode was the same as that for a

#9300 - $15.00 USD Received 28 October 2005; revised 30 November 2005; accepted 21 December 2005

plasma slab [33], yet the PPW TM_1 mode was different from that for a dielectric slab [34], which may be due to the negative dielectric cladding of the DPG.

Whereas the above TM_0 modes were always forward type, the TM_1 modes could also be backward waves, as indicated by negative slopes on the curves, when the gap widths were narrow, as shown in Figs. 2(c)-(f). As such, among the six gap widths in Fig. 2, the TM_1 mode for $h = 15$ nm (Fig. 2(c)) had a very narrow frequency band for propagating, while the others all had relatively wider regimes. Despite the dissimilar structures [17, 38-41] and media [42-45], the backward wave properties here were essentially the same in principle, and mainly caused by vortex-like Poynting vectors along the interface between the two different media with opposite signs [43-45].

As shown in Fig. 2, the TE_1 modes had identical cutoff frequencies to the TM_1 modes. The TE_1 mode was always a forward wave type, while the TM_1 mode could have both types, depending on the gap width. From Table 1, the characteristic equation for the TE_1 mode included $\tan(\cdot)$, while the TM_1 modes included $\cot(\cdot)$. Yet, a TM_1 mode with $\cot(\cdot)$ contradicts the mode assigned to the well-established dielectric slab waveguides, where an odd-numbered mode is symmetrical (tangent function) in its field configurations, while an even-numbered mode is antisymmetrical (cotangent function). Prade *et al*. just indexed "odd" and "even" modes [21], not assigned mode numbers, which was consistent with the dielectric slab case. However, here, identical cutoff frequency between two modes leads us to assign them to same mode number as in the PPW case, whose cutoff frequency of the TE and TM modes are the same. Thus, TE_0 mode here is absent and the first TE mode is the TE_1 mode as is for the case of the dielectric slab waveguides. As shown in the Fig. 2(a), thereby, each of TM and TE modes with $m = 1, 2$, and 3 are very much correlated due to the identical cutoff frequency. In the case of the PEC PPWs, the normalized propagation constants are the same. The relationships in the dispersion curves between the PEC PPW and the DPG will be shown in the next subsection. In Fig. 2(a), higher order modes for $m \geq 2$ cases are plotted in series with an increase of the frequency. Higher order modes are all PPW modes, which are also numerically obtained and plotted with the criteria of the mode number assigning in Table 1.

The cutoff frequency of the TE_1 mode is always below the plasma frequency even at very narrow subwavelength gap width, as shown in the inset of Fig. 2(f). Beginning from the cutoff frequency, which is identical to that of the TM_1 mode, the TE_1 mode is monotonically increased as the frequency increases, even above the plasma frequency seamlessly. At very narrow subwavelength gap conditions, *e.g.*, $h = 1$nm case in Fig. 2(f), the TE_1 mode is never suppressed. This means that not only SPP mode but also PPW TE modes can contribute to the subwavelength guidance. Above the plasma frequency, at least two guided modes always exist even at considerably narrow subwavelength gap conditions; one is TM and the other is TE mode. The TE mode begins always below the plasma frequency, while the TM mode does right at the plasma frequency.

Shaded region beginning from the plasma frequency of $f_c = 3600$ THz is forbidden region, in which any guided mode solutions does not exist. This region is delimited with the refractive index of the cladding (n_2) as dotted lines, as shown in the Fig. 1(b). Above the plasma frequency, there is one propagating TM modes whose normalized propagation constants are slightly higher than the refractive index of the cladding. (So, in the scale of Fig. 2, it is difficult to distinguish n_2 (dotted lines) from β / k_0 of the TM modes. In Fig. 2(c), *i.e.*, $h = 15$ nm case, the propagating mode (TM_2 mode) and the refractive index (n_2) are distinguishable.) Above the plasma frequency, the refractive index of the core is greater than that of the cladding, *i.e.*, $n_1 > n_2$, where $n_1 = 1.0$ and $0.0 < n_2 < 1.0$. This condition is consistent with "index guiding" as in cases of conventional dielectric film guiding or well known optical fibers [46, 47].

As the gap widths decreases, higher order modes are suppressed and the cutoff frequency for $m = 1$ mode increases. At very narrow gap widths, *e.g.*, $h = 1$nm case, the cutoff frequency approached to the plasma frequency. Thus, it is found that the propagations of the TM_1 mode can exist approximately in the frequency region between the critical frequency and the plasma frequency which are corresponding to the frequencies at $\varepsilon_{r2} = -1.0$ and $\varepsilon_{r2} = 0.0$ cases,

#9300 - $15.00 USD Received 28 October 2005; revised 30 November 2005; accepted 21 December 2005

respectively. Ideally, there exist propagating modes along the DPGs at considerably narrow subwavelength gaps; the forward TM_0 mode in the SPP region from DC to critical frequency, the backward TM_1 mode both in the SPP and the PPW modes from the critical frequency to the plasma frequency, and the forward TE_1 and TM_2 modes in the PPW mode above the plasma frequency.

3.2 Relations with PEC PPW

Usually, metals in waveguides are ideally assumed to be PECs, while the metal in the DPGs here has the plasmonic response. However, there are some connections between the DPGs and the PEC PPWs. Mode numbers assigned to the DPGs in the previous subsection were in consistency with the PEC PPWs. In Fig. 3, normalized propagation constants of the PEC PPWs for $h = 50$ and 25 nm are plotted with those of the DPGs. Normalized propagation constant of the PEC PPW for the TM_m/TE_m ($m \geq 1$) mode is given as follows [34].

$$\bar{\beta} = \frac{\beta}{k_0} = \left\{ 1 - \left(\frac{m\pi}{2k_0 h} \right)^2 \right\}^{1/2} \qquad (1)$$

In cases of much narrower gap widths, the cutoff frequencies between the PEC PPW and the DPGs are located very far from each other along the frequency axis, *i.e.*, the cutoff frequencies of the PEC PPWs are very much higher than those of the DPGs and the comparisons between them are meaningless. As shown in the Fig. 3, the cutoff frequencies of the DPGs were decreased in comparison with those of the PEC PPWs. This allows the propagation along the DPGs possible even when the mode of the PEC PPWs cannot exist. We observed that the difference of the cutoff frequencies between the PEC PPWs and DPGs in dispersion curves became greater as the increases of the mode numbers and the decreases of the gap widths. In spite of the different structures, the decreases of the cutoff frequency can also be found in other SPP propagating structures [11, 12]. The dispersion curves of the TE and TM modes for the PEC PPWs are identical, but those for the DPGs split each other due to the plasmonic response of the cladding medium. Especially, the TM_0 and TM_1 modes are quite different from the higher order modes ($m \geq 2$).

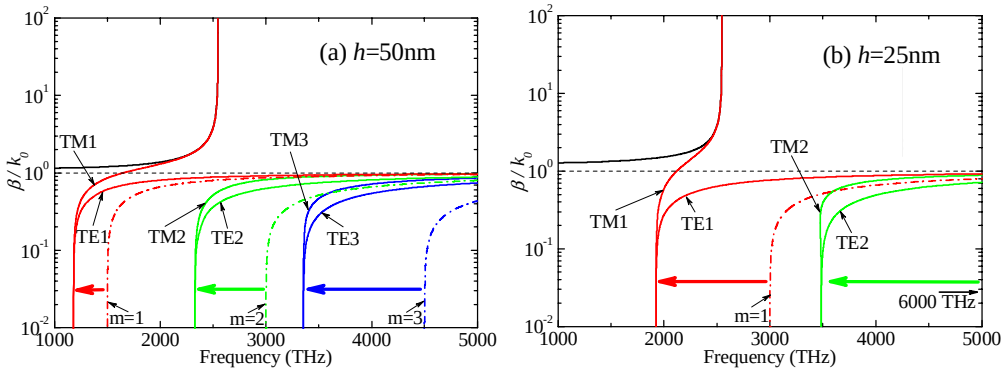

Fig. 3. Dispersion curves for DPG waveguides, plus PEC versions. (a) $h = 50$nm and (b) $h = 25$nm . The curves are the same as those shown in Fig. 2, with the addition of dispersion curves for PEC PPWs, represented by dotted and dashed lines. The dispersion curves for the TM_m/TE_m modes of the PEC PPWs are identical. The arrows depict the decreases in the cutoff frequencies. In (b), 6000 THz is the cutoff frequency for the TM_2/TE_2 mode.

3.3 Surface plasmon polariton (SPP) modes

Figure 4 shows the gap width dependence of the SPP dispersion characteristics of the DPGs for more obvious contrasts. As mentioned above, the SPPs of the DPGs have two distinct TM_0

#9300 - $15.00 USD Received 28 October 2005; revised 30 November 2005; accepted 21 December 2005

and TM_1 modes, which are ones of the essential subwavelength light guidance modes. (The other subwavelength guiding mode is the TE_1 mode, which is limited to higher frequency regime in its existence.) As shown in Table 1, the SPP modes are directly influenced by the signs of the media, *i.e.*, $\varepsilon_{r2} < 0$. The TM_0 mode exists only below the critical frequency with forward wave type, as mentioned above. As the gap widths are decreased, the normalized propagation constants are increased, which means that more power penetrates to the negative cladding region in the evanescent form. Thus, the phase velocity of the modes becomes slower. The reason why the TM_0 mode keeps the forward wave even when the gap width is very narrow is that the power flow along the core region is always greater than that of the cladding region. Whereas the TM_0 mode has high frequency cutoff at the critical frequency, the TM_1 mode can reside both below and above the critical frequency. For the TM_1 mode, as shown in Fig. 4(b), decreases of the gap widths make the mode backward waves from the forward waves. At relatively wider gap widths, *e.g.*, $h = 50$ or 25 nm cases, the TM_1 modes are forward waves with positive slopes in the dispersion curves. However, for narrower gaps, bifurcation points came into being and backward waves existed, which means that the power flow along the cladding region becomes more dominant compared with those along the core region. Inset of the Fig. 4(b) shows the position of the bifurcation points, at which the slopes of the dispersion curves change from negative (corresponding to the backward waves) to positive (corresponding to the forward waves), or vice versa. The dispersion curves of the SPP modes of varied gap widths are tightly bound to the critical frequency. This is essentially due to the frequency dependent nature of the plasmonic medium which is fitted to the classical Drude model, *i.e.*, $\varepsilon(\omega) = 1 - \omega_p^2 / \omega^2$.

#9300 - $15.00 USD Received 28 October 2005; revised 30 November 2005; accepted 21 December 2005

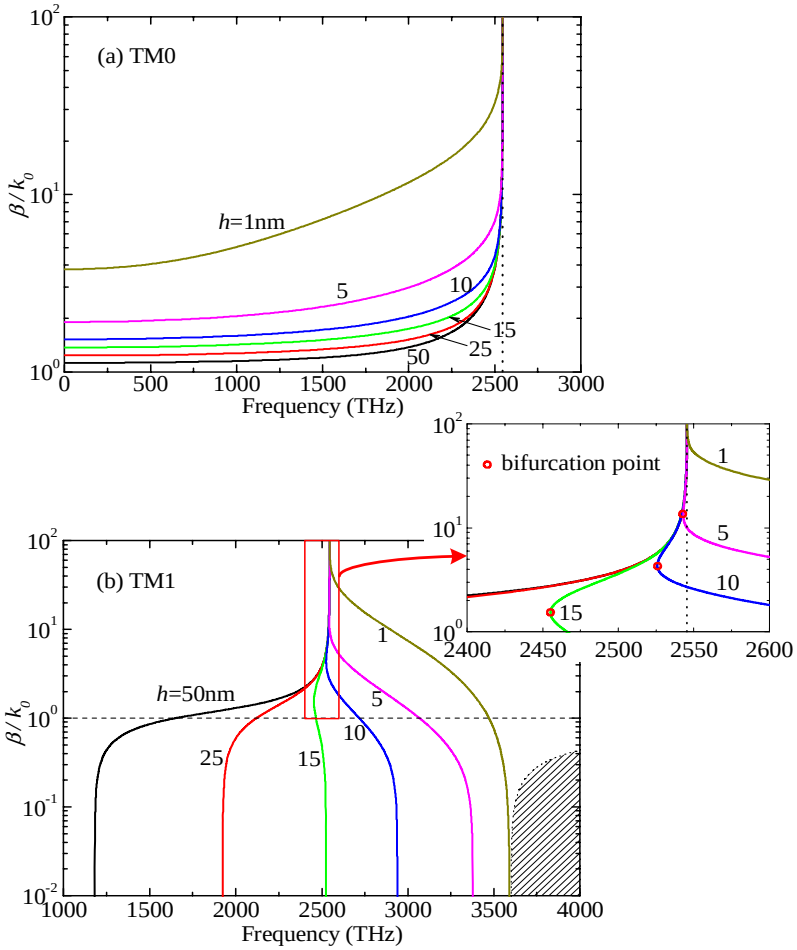

Fig. 4. Dispersion curves for SPP modes of DPGs. (a) TM_0 mode and (b) TM_1 mode. The vertical dotted lines represent the position of the critical frequency, *i.e.*, 2545.58 THz. The bifurcation points in the inset are the frequency points where the forward and backward waves meet.

4. Conclusions

Light transmission along the DPG is numerically investigated and their dispersion characteristics are analyzed with an emphasis on its subwavelength guidance characteristics. Evolutions of the entire guided modes with respect to the varied gap widths are shown and contrasted, from which salient views of the role of the gap widths on the dispersion characteristics of the DPGs are obtained. Proper mode numbers are assigned to the characteristic equations in order to be in consistency with PEC PPWs. At considerably narrow subwavelength gap widths, the TM_1 mode existed approximately within the region between the critical frequency and the plasma frequency over the fast (PPW mode) and slow (SPP mode) wave regions. The TM_0 mode resided below the critical frequency within the SPP mode region and the TM_2 mode resided above the plasma frequency within the PPW mode region. The TE_1 mode of the PPW mode are also supportable, whose cutoff frequency is always below the plasma frequency. Decreased cutoff frequencies of the DPGs, which were compared with those of the PEC PPWs, were also observed. Since the modern advanced nanoscale fabrication techniques allow us to engineer very compact nanophotonic devices, fundamental research results here are expected to be applied to the design guidelines in other nanophotonic or subwavelength device applications.

#9300 - $15.00 USD Received 28 October 2005; revised 30 November 2005; accepted 21 December 2005

Acknowledgments

This work was supported by grant No. R01-2004-000-10158-0 from the Basic Research Program of the Korea Science & Engineering Foundation.

#9300 - $15.00 USD Received 28 October 2005; revised 30 November 2005; accepted 21 December 2005